Rod separation by sawtooth channel

H. Karimi,[1,*] M. R. Setare,[1,†] and A. Moradian[2,‡]
[1]*Department of Science, University of Kurdistan, Sanandaj, Iran*
[2]*Department of Science, Campus of Bijar, University of Kurdistan, Bijar, Iran*

(Received 12 May 2020; accepted 9 July 2020; published 27 July 2020)

By applying entropic barriers, we present a rod separation mechanism that induces the movement of rods of different sizes in the opposite directions. This mechanism is based on the combination of the saw-tooth channel, a static force, and an oscillating driving force. The asymmetric shape of the channel and the elongated shape of the rod causesa complicated interaction effect between the rods and the channel walls which reduces the accessible configuration space for the rods and leads to entropic free-energy effects.

DOI: 10.1103/PhysRevE.102.012610

I. INTRODUCTION

Infiltration in microstructures such as porous media [1–5], micro- or nanofluid channels [6–10], and living tissues [11,12] is an important problem and has attracted the attention of physicists, mathematicians, biologists, and engineers. A common property of these systems is walls of irregular shapes which restrict the motion of the particles. One of the important applications of this problem is the separation of particles based on their size. Obtaining pure materials by separating the desired elements from the impure elements is a major challenge in industrial processes and fundamental research. Particle separation techniques take advantage of the fact that the reaction of particles to an external excitation, for example, fields, depends on their size [13]. Reguera and co-workers presented a mechanism for spherical particle separation [13]. In this paper, we present a mechanism for rod separation that causes rods of different sizes to move in opposite directions and to be sorted by their size.

The axially symmetric particles like rods when moving near a wall experience an additional anisotropic drag force on top of themselves due to their nonspherical shape [14]. Also, the coupling between translation and rotation leads to complicated behavior; for example, colloids [15–19], artificial and biological filaments [3,20], microswimmers [21,22], DNA strands [23,24], and DNA fragments [25] show a complicated coupling between translation and rotation.

The rest of the article is organized as follows: In Sec. II we investigate the dynamics of a suspended rod in a fluid. In Sec. III we present the mechanism of rod separation using a saw-tooth channel, and finally, we present general conclusions in Sec. IV.

II. ROD DYNAMICS

In this section we investigate the rod dynamics under a static force f and an oscillating force $F(t)$, assuming the rod's density is diluted and immersed in a fluid with strong viscosity at low Reynolds number dynamics. In the rod motion, structural constraints produce anisotropy, and the presence of walls leads to a general velocity decrease of Brownian motion due to hydrodynamic interactions of the diffusing rods with walls [26]. The diffusion coefficient is given by the Einstein relation

$$D = K_B T M = \frac{K_B T}{\gamma}, \tag{1}$$

where K_B is the Boltzmann constant, T is temperature, and γ and M are friction coefficient and hydrodynamic mobility of a rodlike particle, respectively. The tensor form of D is $\mathbb{D}_{IJ} = K_B T \mathbb{M}_{IJ} = K_B T/\Gamma_{IJ}$ with $I, J = X, Y, \theta$, where $\mathbb{M}_{IJ}$ and Γ_{IJ} are the tensor form of M and γ, respectively. Here the coordinates X, Y refer to the rod body frame, and θ is the angle between direction of the rod (X axis) and the x axis, where the coordinates x, y, z refer to the laboratory frame (see Fig. 1, left). The diffusion tensor is given by

$$\mathbb{D}_{IJ} = \begin{pmatrix} \mathbb{D}_{XX} & \mathbb{D}_{XY} & \mathbb{D}_{X\theta} \\ \mathbb{D}_{YX} & \mathbb{D}_{YY} & \mathbb{D}_{Y\theta} \\ \mathbb{D}_{\theta X} & \mathbb{D}_{\theta Y} & \mathbb{D}_{\theta\theta} \end{pmatrix} = K_B T \begin{pmatrix} \Gamma_{XX} & \Gamma_{XY} & \Gamma_{X\theta} \\ \Gamma_{YX} & \Gamma_{YY} & \Gamma_{Y\theta} \\ \Gamma_{\theta X} & \Gamma_{\theta Y} & \Gamma_{\theta\theta} \end{pmatrix}^{-1}. \tag{2}$$

The transformation matrix from the rod body to the laboratory frame is

$$\mathbb{R} = \begin{pmatrix} \cos\theta & -\sin\theta & 0 \\ \sin\theta & \cos\theta & 0 \\ 0 & 0 & 1 \end{pmatrix}. \tag{3}$$

The diffusivity in the rod body frame is measured by the displacement covariance matrix (normal diffusion): $2\mathbb{D}_{IJ}\delta t = \langle \delta I \delta J \rangle$ [27]. For example, $\mathbb{D}_{XX} = \langle \delta X^2 \rangle / 2\delta t$ or $\mathbb{D}_{X\theta} = \langle \delta X \delta\theta \rangle / 2\delta t$. The transition $\mathbb{D}_{IJ}$ from the rod body to the laboratory frame is applied by

$$\mathbb{D} = \mathbb{R}\mathbb{D}^{\text{rod}}\mathbb{R}^{\mathbb{T}}, \tag{4}$$

*ha.karimi@sci.uok.ac.ir
†rezakord@ipm.ir
‡a.moradian@uok.ac.ir

 ©2020 American Physical Society

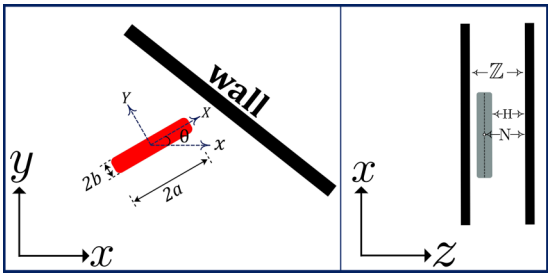

FIG. 1. (Left: side view) Schematic illustration of a rod adjacent to a wall. The coordinates x, y, z and X, Y refer to the laboratory and rod body frames, respectively, and θ is the angle between the direction of the rod (X axis) and the x axis (variable between $+\pi/2$ and $-\pi/2$). $2a$ and $2b$ are rod length and width, respectively. (Right: top view) Schematic illustration of a rod between two parallel walls. $\mathbb{Z}$ is the distance between two walls along the z axis, which has a value of about $2b_{\max}(\mathbb{Z} = 2b_{\max} + \delta\mathbb{Z})$, H is the distance between the wall and the edge of the rod, and N is the distance between the wall and the rod center ($N = H + b$).

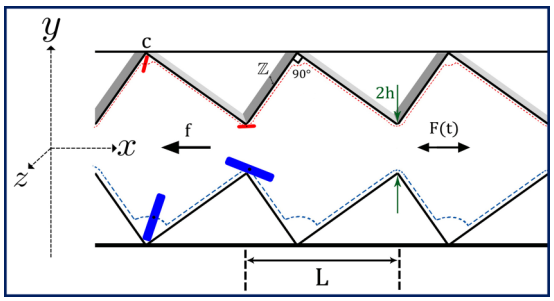

FIG. 2. Schematic illustration of the quasi-two-dimensional channel that restricts the rods' movement. The walls' structure is determined by Eq. (12). The rods are driven by a constant force f and an oscillating force $F(t)$ (e.g., a square wave) along the main axis of the channel. The dashed blue (red) line represents the limit for the positions of the largest (smallest) rod center inside the channel. h is the half-width of the bottleneck, c represents the location of a point with the maximum width, L is the periodicity of the channel, and $\mathbb{Z}$ is the channel thickness along the z axis.

where $\mathbb{D}$ and $\mathbb{D}^{\text{rod}}$ refer to the diffusion tensor in the laboratory and rod body frame, respectively, and $\mathbb{T}$ denotes the matrix transpose.

For a single rod confined between two parallel walls with distance $\mathbb{Z}$, the lateral diffusion in the rod body frame can be described by [28]

$$\mathbb{D}^{2w}(N, p, \mathbb{Z}) = \mathbb{D}^{\text{bulk}}(p) f^{2w}(N, b, \mathbb{Z}), \tag{5}$$

where $p = a/b$ is rod aspect ratio and N is the distance between the wall and the rod center (see Fig. 1, right). $\mathbb{D}^{\text{bulk}}(p)$ is diffusion in the unbounded space, and the simplest approximation solution for $f^{2w}(N, b, \mathbb{Z})$, suggested by Oseen [26], is

$$f^{2w}(N, b, \mathbb{Z}) = \left[\frac{1}{f^{1w}(N, b)} + \frac{1}{f^{1w}(\mathbb{Z} - N, b)} - 1\right]^{-1}, \tag{6}$$

which includes the effects of both walls. Here $\mathbb{D}^{\text{bulk}}(p)$ and $f^{1w}(N, b)$ are determined by the following relations for $H < b$ and $6 < p < 16$ [29]:

$$\mathbb{D}_{\parallel}^{\text{bulk}}(p) = \frac{K_B T}{2\pi\eta 2a}\left[\ln(p) + \frac{-1.951p^2 - 9.132p + 69.16}{p^2 + 39p + 44.4}\right], \tag{7}$$

$$\mathbb{D}_{\perp}^{\text{bulk}}(p) = \frac{K_B T}{4\pi\eta 2a}\left[\ln(p) + \frac{-0.3604p^2 + 28.36p + 72.63}{p^2 + 36.29p + 34.9}\right], \tag{8}$$

$$f_{\parallel}^{1w}(N, b) = \frac{0.9909\left(\frac{N}{b}\right)^3 + 0.3907\left(\frac{N}{b}\right)^2 - 0.1832\left(\frac{N}{b}\right) - 0.001815}{\left(\frac{N}{b}\right)^3 + 2.03\left(\frac{N}{b}\right)^2 - 0.3874\left(\frac{N}{b}\right) - 0.07533}, \tag{9}$$

$$f_{\perp}^{1w}(N, b) = \frac{0.9888\left(\frac{N}{b}\right)^3 + 0.788\left(\frac{N}{b}\right)^2 - 0.207\left(\frac{N}{b}\right) - 0.004766}{\left(\frac{N}{b}\right)^3 + 3.195\left(\frac{N}{b}\right)^2 - 0.09612\left(\frac{N}{b}\right) - 0.1523}, \tag{10}$$

where η is the fluid medium viscosity and $\parallel$ ($\perp$) denotes parallel (perpendicular) to the long axis of the rod. In Eqs. (9) and (10), instead of N, we put $\mathbb{Z} - N$, to obtain $f^{1w}(\mathbb{Z} - N, b)$.

Since the inertial forces of the rod are negligible with respect to the viscous forces, we use overdamped Langevin equations to describe the rod dynamics [27,30]:

$$\frac{d\vec{r}}{dt} = \frac{\mathbb{R}\mathbb{D}^{2w}\mathbb{R}^{\mathbb{T}}}{K_B T}[f^{\text{rod}} + F^{\text{rod}}(t)]\vec{e}_x + \sqrt{\mathbb{R}\mathbb{D}^{2w}\mathbb{R}^{\mathbb{T}}}\vec{\xi}(t), \tag{11}$$

where $\vec{r}$ is the rod center vector (in a laboratory frame) and $\vec{e}_x$ is the unit vector along the x direction. f^{Rod} and F^{Rod} are the forces applied to the rod. Fluctuations in the rod body frame are "independent Gaussian white noises," $\vec{\xi}(t)$, with zero mean, $\langle\vec{\xi}(t)\rangle = 0$, and $\langle\xi_I(t)\xi_J(t + t')\rangle = 2\delta_{IJ}\delta(t')$ for $I, J = X, Y, \theta$ [27].

III. MECHANISM OF ROD SEPARATION BASED ON THEIR SIZE

In this section, we present a mechanism for rod separation using a saw-tooth channel. The principles of this mechanism rely on the combination of a driving force and an entropic rectification [31–34]. In an asymmetric structure, the entropic potential becomes asymmetric. In this structure, we can create a rectification to the right direction by a zero-mean oscillating force and select a specific structure where the entropic barriers in the left direction are larger than those in the right direction. The strength of this rectification depends on the rod's size. For large rods, the entropic barrier is larger, so the strength is stronger. Thus, in the presence of a static force f applied in the left direction, the small rods follow the static force while the large rods move in the opposite direction under the influence of rectification, and rods of different sizes can be separated. To illustrate this effect, we choose a quasi-two-dimensional saw-tooth channel (see Fig. 2), where rods are affected by a static force f and an oscillating force $F(t)$ so that both forces are applied along the main axis of the channel. The reason for choosing a quasi-two-dimensional channel

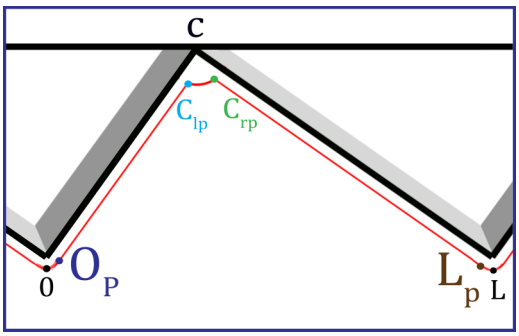

FIG. 3. Illustration of the channel wall, the intersection points, and the limit of the position of the rod center near the wall.

(not three-dimensional) is the anisotropic drag coefficients for rod diffusion inherently increase when the rods are hardly restricted between parallel walls [35]. In the quasi-2D confinement, the effects of entropic barriers on the rods increase when the rod aspect ratio, p, increases and contribute to a faster separation.

For the sake of the simplicity, we obtain the channel structure in two dimensions (the x-y plane). The upper wall of channel reads

$$y_{\rm up}(x) = \begin{cases} h + m_1\bar{x}, & \text{if } \bar{x} < \text{c} \\ h + m_2(L - \bar{x}), & \text{otherwise} \end{cases}, \tag{12}$$

where h is the half-width of the bottleneck, m_1 and m_2 are the slopes of the walls, L is the periodicity of the channel, and $c = Lm_2/(m_1 + m_2)$ represents the location of a point with the maximum width. We choose the slopes of the walls in order to have an angle of 90° in the point c, i.e., $m_1 * m_2 = 1$, where $m_1 > m_2$. The bottom wall of the channel $y_{\rm bottom}(x) = -y_{\rm up}(x)$, and $\bar{x}$ denotes x inside a L period (to create a periodic structure).

For a hard rod with half-width b and half-length a inside the channel, the space available for its center is restricted as

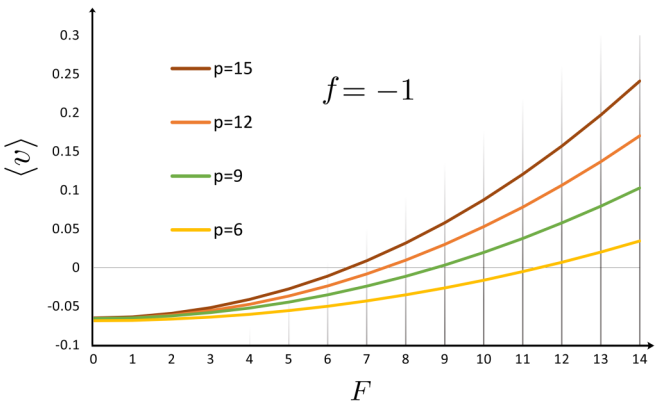

FIG. 4. Average current vs the periodic force F for rods of different aspects, for a channel with $m_1 = 4$, $m_2 = 1/4$, $h = 1.6$, $\mathbb{Z} = 0.35$, $L = 14$ and the rod with $b = 0.1$. For $f < 0$ small rods move to the left, whereas large rods move to the right. The critical aspect that determines these two behaviors can be tuned by the values of F and f. The critical force that determines velocity inversion depends on the rod length a.

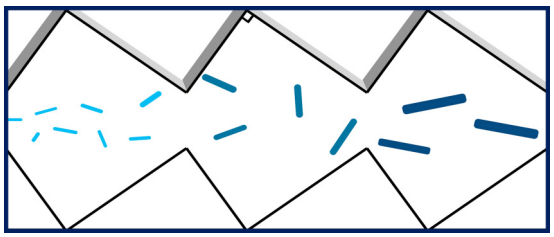

FIG. 5. Schematic illustration of rods of different sizes inside the channel where they are initially placed in the middle of the channel, and after the forces were applied, the large rods moved to the right and the small rods to the left.

follows:

$$\mathbb{W}(x)_{\rm up} = \begin{cases} -\sqrt{b^2 - \bar{x}^2} + h, & 0 \leqslant \bar{x} < O_p \text{ (a)} \\ h + m_1\bar{x} - b\sqrt{1 + m_1^2}, & O_p \leqslant \bar{x} < c_{lp} \text{ (b)} \\ -\sqrt{a^2 - (\bar{x} - c)^2} + h + m_1 c, & c_{lp} \leqslant \bar{x} < c_{rp} \text{ (c)}, \\ h + m_2(L - \bar{x}) - b\sqrt{1 + m_2^2}, & c_{rp} \leqslant \bar{x} < L_p \text{ (d)} \\ -\sqrt{b^2 - (\bar{x} - L)^2} + h, & L_p \leqslant \bar{x} < L \quad \text{(e)} \end{cases} \tag{13}$$

where O_p is the intersection point of curve (a) with line (b), $O_p = bm_1/\sqrt{1 + m_1^2}$, c_{lp} is the intersection point of line (b) with curve (c), $c_{lp} = c + (bm_1 - \sqrt{a^2 - b^2})/\sqrt{1 + m_1^2}$, c_{rp} is the intersection point of the curve (c) with line (d), $c_{rp} = c + (\sqrt{a^2 - b^2} - bm_2)/\sqrt{1 + m_2^2}$, and L_p is the intersection point of line (d) with curve (e), $L_p = L - (bm_2)/\sqrt{1 + m_2^2}$. The bottom parallel curve is $\mathbb{W}_{\rm bottom}(x) = -\mathbb{W}_{\rm up}(x)$. As a result, the local width of the structure accessible for the rod center becomes $2\mathbb{W}(x) = \mathbb{W}_{\rm up}(x) - \mathbb{W}_{\rm bottom}(x)$. Figure 3 shows how the channel walls limit the space for the rod center.

According to our assumptions in this paper, we neglect all the hydrodynamic rod-rod interactions. The times of equilibrium along y and the rotation of rod, θ, are sufficiently short (i.e., τ_y, $\tau_\theta \ll \tau_x$ where τ_y, τ_θ, and τ_x are diffusion times along the y, θ, and x directions, respectively), so we can integrate the probability density function $\rho(x, y, \theta, t)$ to obtain $P(x, t) =$

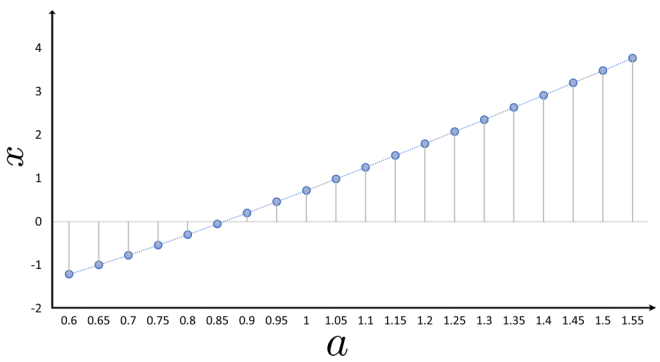

FIG. 6. The position of the rods' center with different lengths and the same widths ($b = 0.1$) after 60 sec. First, the rods were at $x = 0$, and after 60 sec, the rods were separated.

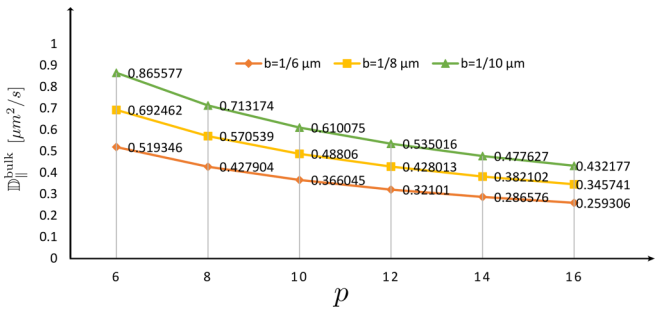

FIG. 7. Translational diffusion parallel to the long axis in the unbounded space vs aspect ratio, for three widths, $b = 1/6, 1/8, 1/10\,\mu$m.

$\iint \rho(x, y, \theta, t)\, dy\, d\theta$ [27], where $P(x, t)$ is the probability of the rod's existence in a cross section, at position x and time t. The description of this system can be given by the concept of an entropic potential [36]. The rod diffusion in the channel can be described by the Fick-Jacobs (FJ) free energy. Consequently, the corresponding FJ equation of Eq. (11) for the distribution function at position x is [36–39]

$$\frac{\partial P(x,t)}{\partial t} = \frac{\partial}{\partial x}\left\{D(x)\left[\frac{\partial}{\partial x}P(x,t) + P(x,t)\frac{1}{K_B T}\frac{\partial}{\partial x}\mathbb{V}(x)\right]\right\}, \tag{14}$$

where

$$\mathbb{V}(x) = U - TS(x) = -[f^{\text{rod}} + F^{\text{rod}}(t)]x - TK_B \ln[2\mathbb{W}(x)] \tag{15}$$

is free energy and $S(x) = K_B \ln[2\mathbb{W}(x)]$ is the entropy. $D(x)$ is an effective longitudinal diffusivity function, which we will obtain below.

Given that after the forces are applied along the x axis, the rod density increases around $y = 0$ [40], and long relaxation time in the longitudinal coordinate relative to the transverse and rotational relaxation times, we conclude that diffusion will be dominated along the x axis. From $\mathbb{D} = \mathbb{R}\mathbb{D}^{\text{rod}}\mathbb{R}^{\mathbb{T}}$, and neglecting off-diagonal elements of $\mathbb{D}^{\text{rod}}$, the element of diffusivity matrix along the main axis of the channel, $\mathbb{D}_{xx}$, is obtained,

$$\mathbb{D}_{xx}^{2\text{w}} = \mathbb{D}_{XX}^{2\text{w}} \cos^2\theta + \mathbb{D}_{YY}^{2\text{w}} \sin^2\theta, \tag{16}$$

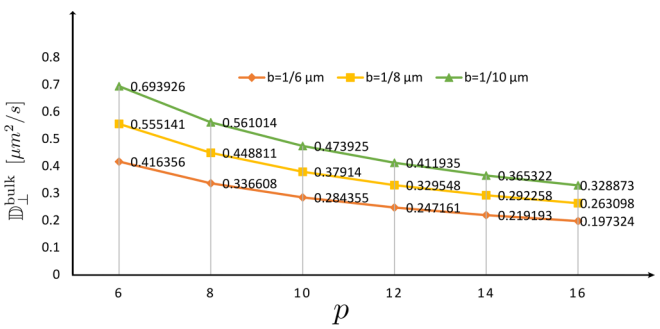

FIG. 8. Translational diffusion perpendicular to the long axis in the unbounded space vs aspect ratio, for three widths, $b = 1/6, 1/8, 1/10\,\mu$s.

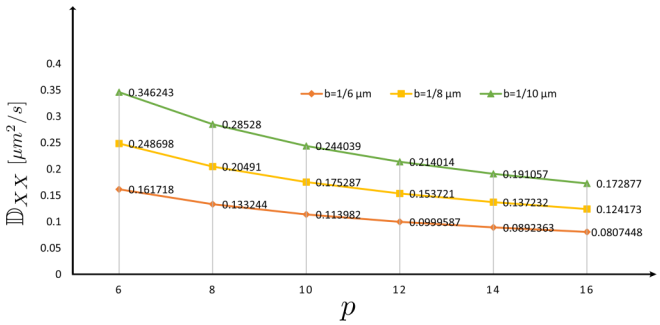

FIG. 9. XX element of a translational diffusion tensor confined between two parallel walls with distance $\mathbb{Z}$, vs aspect ratio, for three widths, $b = 1/6, 1/8, 1/10\,\mu$m.

from Eqs. (5) and (6):

$$\mathbb{D}_{XX}^{2\text{w}} = \mathbb{D}_{\parallel}^{\text{bulk}}(p)\left[\frac{1}{f_{\parallel}^{1\text{w}}(N,b)} + \frac{1}{f_{\parallel}^{1\text{w}}(\mathbb{Z}-N,b)} - 1\right]^{-1}, \tag{17}$$

$$\mathbb{D}_{YY}^{2\text{w}} = \mathbb{D}_{\perp}^{\text{bulk}}(p)\left[\frac{1}{f_{\perp}^{1\text{w}}(N,b)} + \frac{1}{f_{\perp}^{1\text{w}}(\mathbb{Z}-N,b)} - 1\right]^{-1}. \tag{18}$$

We obtained the values of $\mathbb{D}^{2\text{w}}$ and $\mathbb{D}^{\text{bulk}}$ for certain cases analytically in the Appendix.

When the rods get very close to the boundaries, they are reflected due to boundary conditions, and the orientation of the longer rods in the channel bottleneck around the $\theta = 0$ is constrained [27] (note that, to prevent the channel bottleneck from being blocked, we must have $2a_{\max} < 2h$). But in the middle of the channel cells, the rod can experience any angle θ. However, using an approximation for near the boundaries, we assume that the probability of the rod angles across the channel is equal, then by averaging Eq. (16) over θ, $D_{\text{ave}}^{2\text{w}} = \langle \mathbb{D}_{xx}^{2\text{w}} \rangle_{\theta}$, and replacing $D_{\text{ave}}^{2\text{w}}$ in the Rubi and Reguera expression in Ref. [36] for a two-dimensional structure and an approximation used in Ref. [27], $D(x)$ is obtained:

$$D(x) = \frac{D_{\text{ave}}^{2\text{w}}}{[1 + \mathbb{W}'(x)^2]^{\frac{1}{3}}}, \tag{19}$$

where the prime refers to the derivative with respect to x.

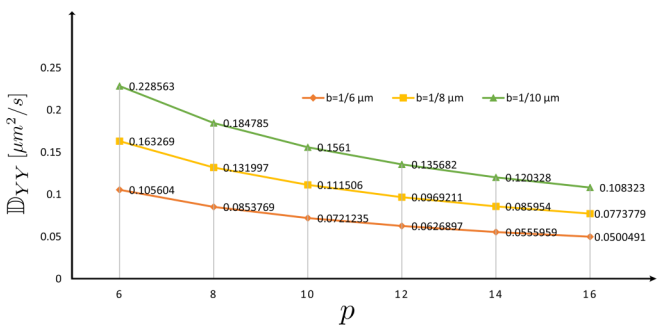

FIG. 10. YY element of translational diffusion tensor confined between two parallel walls with distance $\mathbb{Z}$, vs aspect ratio, for three widths, $b = 1/6, 1/8, 1/10\,\mu$m.

For the sake of a dimensionless description, we introduce three parameters: the length L, energy K_BT, and diffusion time along the main axis of the channel, $\tau_x = L^2/D^{2w}_{ave}(\min)$. Then free energy and effective diffusivity being dimensionless, respectively, become $\widetilde{\mathbb{V}}(x) = -[f^{rod} + F^{rod}]x - \ln[2\mathbb{W}(x)]$ and $\widetilde{D}(x) \simeq (h+H+b)/\{(a+N)[1+\mathbb{W}'(x)^2]^{\frac{1}{3}}\}$. Here $D^{2w}_{ave} \simeq D^{2w}_{ave}(\min)(h+H+b)/(a+N)$, where $D^{2w}_{ave}(\min)$ is the diffusion coefficient of a rod with $a \simeq h$ and $2b \simeq \mathbb{Z}$. The forces applied to the rods in the fluid depend on the rods' aspect, so we will consider $f^{Rod} = fa/h$ and $F^{Rod} = Fa/h$.

Using the Stratonovich's formula, the dimensionless current reads [30,41–43]

$$J(F) = \frac{1 - e^{-(F+f)a/h}}{\int_{x_0}^{x_0+1} dz \frac{1}{D(z)} e^{\mathbb{V}(z)} \int_{z-1}^{z} dx\, e^{-\mathbb{V}(x)}}. \qquad (20)$$

In the adiabatic limit, the average velocity becomes $\langle v \rangle = [J(F) + J(-F)]/2$ [13].

Figure 4 indicate the average current of rods for different values of periodic force F. If we apply a small static force f in the left direction, rods larger than a given threshold aspect move to the right, whereas rods smaller than that move to the left. So we can separate rods of different aspect and induce them to move in opposite directions. The reason for this separation is that the large rods are more affected by the applied forces, and the entropic barriers (rectification to the right) only allow the small rods to move to the left. This behavior can be tuned by the value of F and f. The splitting effect is illustrated schematically in Fig. 5.

Now let's consider a sample of 20 rods with the same width and different lengths at the position $x = 0$ and calculate how far the rods will go after 60 sec. To do this, we consider the static force as $f = -1$ and the oscillating force as $F = \pm 9$. Using the obtained velocities (assuming the velocity remains constant) and the time of 60 sec, we obtain the position of the rods according to Fig. 6. As it turns out, the distance from the smallest rod to the largest rod after 60 sec is about five units (for example, a micrometer).

Finally, we make some predictions about the effects of different factors on diffusion. It is preferable to use the small value in periodic force $F(t)$, because at a very high value, the change in the oscillating force is so fast that the rods cannot follow the force, and as a result there is a vanishing effect of the oscillating force [13]. By selecting the channel geometry, the entropy splitter effect can be adjusted, for example, a change the asymmetry of the walls, change in the slopes of the channel walls, or change in the bottleneck width $2h$.

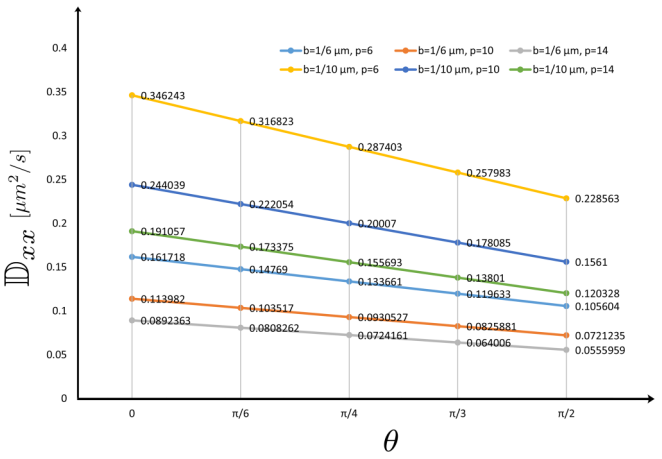

FIG. 11. The element of diffusivity matrix along the main axis of the channel, $\mathbb{D}_{xx}$, vs the angle of the rod, for three aspect ratios, $p = 6$, 10, 14 and two widths, $b = 1/6$, $1/10\,\mu$m.

IV. CONCLUSION

In this paper, we present a mechanism for separating rods based on their size using a saw-tooth channel. This mechanism combines a saw-tooth structure to create entropic barriers and two forces along the main axis of the channel, where f is fixed and $F(t)$ oscillates to create an entropic rectification. This rectification is able to guide the rods in different directions by changing the direction of the rods' movement, and thus they are sorted by their size. The geometrical parameters of the channel and the values of applied forces can be changed more efficiently. This process can be used to separating any rod-shaped object such as DNA strands. This idea can be applied to similar structures such as narrow channels and holes where the entropic effects are prominent.

APPENDIX: DIFFUSION VALUES

We obtain translational diffusion, analytically for a rod in the unbounded space and confined between two parallel walls with distance $\mathbb{Z}$, for several specific parameters in Figs. 7–11. We chose water at a temperature of 293 K as the fluid inside the channel. For the bulk diffusion, we placed the following parameter values in Eqs. (4)–(9): $K_B = 1.38 \times 10^{-23}\,\mathrm{m^2\,kg\,s^{-2}\,K^{-1}}$, $\eta = 10^{-3}\,\mathrm{kg\,m^{-1}\,s^{-1}}$, related to the water of $T = 293$ K, $b_{max} = 1/6\,\mu$m, $b_{min} = 1/10\,\mu$m, and for a rod confined between two parallel walls, $\mathbb{Z} = 0.35\,\mu$m. It is assumed that the rod is trapped almost in the middle of two parallel walls.

[1] B. Berkowitz, A. Cortis, M. Dentz, and H. Scher, Rev. Geophys. **44**, RG2003 (2006).
[2] S. Xu, Q. Liao, and J. E. Saiers, Environ. Sci. Technol. **42**, 771 (2008).
[3] N. Fakhri, F. C. MacKintosh, B. Lounis, L. Cognet, and M. Pasquali, Science **330**, 1804 (2010).
[4] K. He, S. T. Retterer, B. R. Srijanto, J. C. Conrad, and R. Krishnamoorti, ACS Nano **8**, 4221 (2014).
[5] M. J. Skaug, L. Wang, Y. F. Ding, and D. K. Schwartz, ACS Nano **9**, 2148 (2015).
[6] C. Kettner, P. Reimann, P. Hanggi, and F. Muller, Phys. Rev. E **61**, 312 (2000).

[7] S. Matthias and F. Müller, Nature (London) **424**, 53 (2003).
[8] F. Slanina, Phys. Rev. E **94**, 042610 (2016).
[9] X. Yang, C. Liu, Y. Li, F. Marchesoni, P. Hanggi, and H. P. Zhang, Proc. Natl. Acad. Sci. USA **114**, 9564 (2017).
[10] M. J. Skaug, C. Schwemmer, S. Fringes, C. D. Rawlings, and A. W. Knoll, Science **359**, 1505 (2018).
[11] H.-X. Zhou, G. Rivas, and A. P. Minton, Annu. Rev. Biophys. **37**, 375 (2008).
[12] P. C. Bressloff and J. M. Newby, Rev. Mod. Phys. **85**, 135 (2013).
[13] D. Reguera, A. Luque, P. S. Burada, G. Schmid, J. M. Rubi, and P. Hanggi, Phys. Rev. Lett. **108**, 020604 (2012).
[14] M. Lisicki, B. Cichocki, and E. Wajnryb, J. Chem. Phys **145**, 034904 (2016).
[15] Y. Han, A. M. Alsayed, M. Nobili, J. Zhang, T. Lubensky, and A. Yodh, Science **314**, 626 (2006).
[16] F. Hofling, E. Frey, and T. Franosch, Phys. Rev. Lett. **101**, 120605 (2008).
[17] S. Sacanna and D. J. Pine, Curr. Opin. Colloid Interface Sci. **16**, 96 (2011).
[18] A. Chakrabarty, A. Konya, F. Wang, J. V. Selinger, K. Sun, and Q. H. Wei, Phys. Rev. Lett. **111**, 160603 (2013).
[19] D. Kasimov, T. Admon, and Y. Roichman, Phys. Rev. E **93**, 050602(R) (2016).
[20] A. Ward, F. Hilitski, W. Schwenger, D. Welch, A. W. C. Lau, V. Vitelli, L. Mahadevan, and Z. Dogic, Nat. Mater. **14**, 583 (2015).
[21] C. Bechinger, R. Di Leonardo, H. Löwen, C. Reichhardt, G. Volpe, and G. Volpe, Rev. Mod. Phys. **88**, 045006 (2016).
[22] C. Liu, C. Zhou, W. Wang, and H. P. Zhang, Phys. Rev. Lett. **117**, 198001 (2016).
[23] W. Reisner, K. J. Morton, R. Riehn, Y. M. Wang, Z. Yu, M. Rosen, J. C. Sturm, S. Y. Chou, E. Frey, and R. H. Austin, Phys. Rev. Lett. **94**, 196101 (2005).
[24] W. Riefler, G. Schmid, P. S. Burada, and P. Hanggi, J. Phys.: Condens. Matter **22**, 454109 (2010).
[25] M. M. Tirado, C. L. Martínez, and J. G. de la Torre, J. Chem. Phys. **81**, 2047 (1984).
[26] J. Happel and H. Brenner, *Low Reynolds Number Hydrodynamics* (Prentice Hall, Englewood Cliffs, NJ, 1965).
[27] X. Yang, Q. Zhu, C. Liu, W. Wang, Y. Li, F. Marchesoni, P. Hanggi, and H. P. Zhang, Phys. Rev. E **99**, 020601(R) (2019).
[28] J. L. Bitter, Y. Yang, G. Duncan, H. Fairbrother, and M. A. Bevan, Langmuir **33**, 9034 (2017).
[29] Y. Yang and M. A. Bevan, J. Chem. Phys. **147**, 054902 (2017).
[30] H. Risken, *The Fokker-Planck Equation* (Springer, Berlin, 1984).
[31] I. D. Kosinska, I. Goychuk, M. Kostur, G. Schmid, and P. Hänggi, Phys. Rev. E **77**, 031131 (2008).
[32] G. Schmid *et al.*, Adv. Solid State Phys. **48**, 317 (2009).
[33] D. Reguera and J. M. Rubi, Chem. Phys. **375**, 518 (2010).
[34] V. Yu. Zitserman *et al.*, J. Chem. Phys. **135**, 121102 (2011).
[35] Y. Han, A. Alsayed, M. Nobili, and A. G. Yodh, Phys. Rev. E **80**, 011403 (2009).
[36] D. Reguera and J. M. Rubi, Phys. Rev. E **64**, 061106 (2001).
[37] R. Zwanzig, J. Phys. Chem. **96**, 3926 (1992).
[38] M. Jacobs, *Diffusion Processes* (Springer, New York, 1967).
[39] D. Reguera, G. Schmid, P. S. Burada, J. M. Rubi, P. Reimann, and P. Hanggi, Phys. Rev. Lett. **96**, 130603 (2006).
[40] P. S. Burada, G. Schmid, D. Reguera, J. M. Rubi, and P. Hanggi, Phys. Rev. E **75**, 051111 (2007).
[41] R. L. Stratonovich, Radiotekh. Elektron. (Moscow) **3**, 497 (1958).
[42] P. Hanggi, P. Talkner, and M. Borkovec, Rev. Mod. Phys. **62**, 251 (1990).
[43] P. Reimann, C. Van den Broeck, H. Linke, P. Hänggi, J. M. Rubi, and A. Perez-Madrid, Phys. Rev. Lett. **87**, 010602 (2001); Phys. Rev. E **65**, 031104 (2002).